Gibbons, S. J., Sørensen, M., Harris, D. B., Ringdal, F. (2007): The detection and location of low magnitude earthquakes in northern Norway using multi-channel waveform correlation. - Physics of the Earth and Planetary Interiors, 160, 3-4, 285-309

DOI: 10.1016/j.pepi.2006.11.008.

The detection and location of low magnitude earthquakes in northern Norway using multi-channel waveform correlation at regional distances[⊗]

Steven J. Gibbons[a,*], Mathilde Bøttger Sørensen[b,1], David B. Harris[c], Frode Ringdal[a]

[a] *NORSAR, PO. Box 53, N-2027 Kjeller, Norway*
[b] *Department of Earth Sciences, University of Bergen, Allegt. 41, N-5007 Bergen, Norway*
[c] *Lawrence Livermore National Laboratory PO. Box 808, Livermore, CA 94550, USA*

Received 31 March 2006; received in revised form 8 November 2006; accepted 20 November 2006

Abstract

A fortuitous sequence of closely spaced earthquakes in the Rana region of northern Norway, during 2005, has provided an ideal natural laboratory for investigating event detectability using waveform correlation over networks and arrays at regional distances. A small number of events between magnitude 2.0 and 3.5 were recorded with a high SNR by the Fennoscandian IMS seismic arrays at distances over 600 km and three of these events, including the largest on 24 June, displayed remarkable waveform similarity even at relatively high frequencies. In an effort to detect occurrences of smaller earthquakes in the immediate geographical vicinity of the 24 June event, a multi-channel correlation detector for the NORSAR array was run for the whole calendar year 2005 using the signal from the master event as a template. A total of 32 detections were made and all but 2 of these coincided with independent correlation detections using the other Nordic IMS array stations; very few correspond to signals detectable using traditional energy detectors. Permanent and temporary stations of the Norwegian National Seismic Network (NNSN) at far closer epicentral distances have confirmed that all but one of the correlation detections at NORSAR in fact correspond to real events. The closest stations at distances of approximately 10 km can confirm that the smallest of these events have magnitudes down to 0.5 which represents a detection threshold reduction of over 1.5 for the large-aperture NORSAR array and over 1.0 for the almost equidistant regional ARCES array. The incompleteness of the local network recordings precludes a comprehensive double-difference location for the full set of events. However, stable double-difference relative locations can be obtained for eight of the events using only the Lg phase recorded at the array stations. All events appear to be separated by less than

[⊗] Disclaimer: This report was prepared as an account of work sponsored by an agency of the United States Government. Neither the United States Government nor any agency thereof, nor any of their employees, make any warranty, express or implied, or assumes any legal liability or responsibility for the accuracy, completeness, or usefulness of any information, apparatus, product, or process disclosed, or represents that its use would not infringe privately owned rights. Reference herein to any specific commercial product, process, or service by trade name, trademark, manufacturer, or otherwise does not necessarily constitute or imply its endorsement, recommendation, or favoring by the United States Government or any agency thereof. The views and opinions of authors expressed herein do not necessarily state or reflect those of the United States Government or any agency thereof.

[*] Corresponding author. Tel.: +47 63805939; fax: +47 63818719.
E-mail address: steven@norsar.no (Steven J. Gibbons).
[1] Now at GFZ Potsdam, Section 5.3, Telegrafenberg, 14473 Potsdam, Germany.

0.5 km. Clear peaks were observed in the NORSAR correlation coefficient traces during the coda of some of the larger events; the local stations confirm that these are in fact aftershocks exhibiting very similar waveforms to the main events. Many of the more marginal correlation detections are not made when the calculations are repeated using shorter signal segments, fewer sensors or more distant stations. We demonstrate in addition how these almost repeating seismic sources have been exploited to detect and measure timing anomalies at individual sites within the arrays and network.

Keywords: Cross-correlation; Detection; Seismic arrays; Aftershocks

1. Introduction

Waveform correlation provides a method of detecting low-magnitude seismic events occurring in the close vicinity of sites at which previous events have generated high-quality, representative waveforms (*Gibbons and Ringdal*, 2006 and references therein). Correlation or matched filter detectors combine high sensitivity with a low false alarm rate since waveforms recorded at a given station are specific to a very limited source region (see, for example, *Geller and Mueller*, 1980). This property however also leads to the correlation detector's greatest drawback; it can only be applied in situations in which the form of the anticipated waveform is essentially known a priori, and it is still an open question as to how many monitoring situations exist where correlation detectors can reduce significantly the detection threshold for low magnitude seismic events. The proportion of events, which are "repeating sources" is proving to be surprisingly high, in at least some regions (*Schaff and Waldhauser*, 2005; *Schaff and Richards*, 2004a,b). Whilst providing optimism for the applicability of a class of detectors that is entirely reliant upon waveform similarity between events, a number of questions require further investigation. For example, how far from a master event can a subsequent event be such that it can still be detected using waveforms from the master event as a template? Also, to what degree can the source mechanism and magnitude of two events vary whilst still resulting in a correlation detection? The answers to these questions are likely to be strongly dependent upon the geology at the source and on the path (see, for example, *Nakahara*, 2004) and the performance of correlation detectors is likely to vary greatly from region to region.

The international monitoring system (IMS) of the comprehensive nuclear-test-ban treaty organisation (CTBTO) is a sparse worldwide network of sensors installed in order to detect possible clandestine underground nuclear explosions which would constitute a violation of such a treaty. Seismic stations constitute a large component of the IMS and, given the demonstrable improvement in signal detectability which correlation detectors can provide over standard energy detectors, it is highly desirable to supplement the existing detection algorithms with sensitive and robust fully-automatic real-time correlation detectors in order to identify the occurrence of recognized signals wherever possible. In many circumstances, the motivation will be to ascribe with a high degree of confidence a detected signal to a known industrial source (see, for example *Harris*, 1991; *Rivière-Barbier and Grant*, 1993) such that analyst resources are not wasted upon identifying signals from uninteresting sources. Using waveform similarity to identify automatically aftershocks from major earthquakes is also desirable since the location of multiple events in long aftershock sequences can be very time-consuming and can lead to long delays in the production of comprehensive seismic bulletins. However, the primary motivation of this paper is to investigate the detectability (using matched filter detectors) of events which are too weak to be detected using conventional energy detectors at the distances imposed by the limitations of a sparse international network.

Many IMS seismic stations are arrays and *Gibbons and Ringdal* (2006) demonstrate how applying waveform correlation at multiple sites lowers the detection threshold significantly. Continuous correlation coefficient traces for different sites in a seismic array or network can be beamformed to give a single correlation function providing a significant array-gain. Unlike in traditional beamforming, where the channels are delayed according to the anticipated arrival time of a given phase,

correlation coefficient traces are delayed simply according to the definition of the waveform templates. If the signal templates for different sites of a multi-channel matched filter detector all begin simultaneously, and the master and detected events are co-located, a zero-delay beam is applied regardless of the direction from which the signals arrive. Significantly, correlation coefficient traces are coherent over large aperture arrays and networks even when the actual waveforms are not. In the current paper, we will focus on the NORSAR array in Southern Norway (designated PS27 of the IMS). The large inter-site distances in this array, originally designed for the detection of weak teleseismic signals (*Bungum et al.*, 1971), make the processing of regional phases by conventional means notoriously difficult due to the lack of waveform coherence across the array. Since waveform coherence is not a requirement for array-processing of correlation coefficient traces, the techniques presented here are readily applied to the NORSAR array and the results apply equally to seismic networks.

In addition to using waveform correlation for

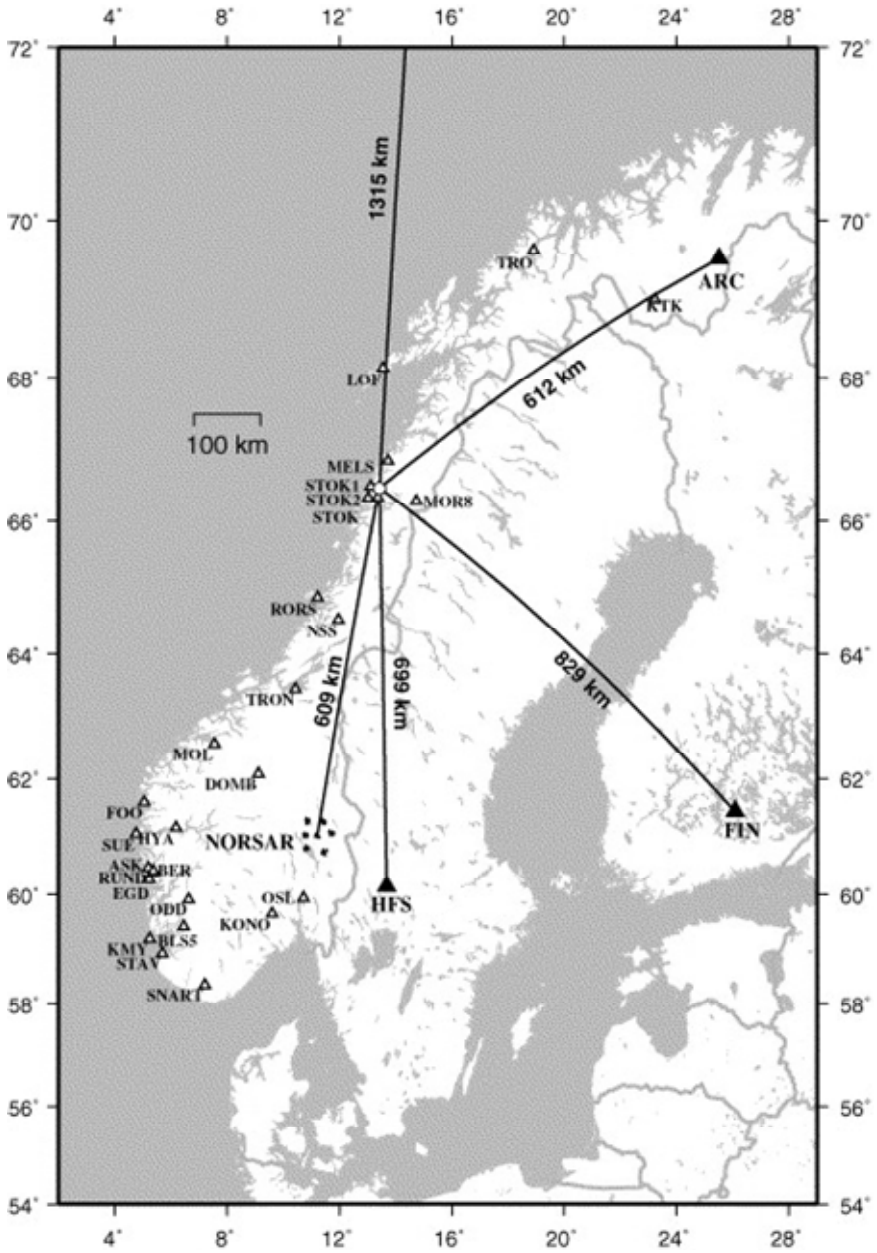

Fig. 1. Location of the 24 June 2005, earthquake in the Rana district of Norway in relation to stations of the NNSN (white triangles) and the Fenno-scandian IMS arrays (black triangles). The line leading northwards leads to the Spitsbergen array, SPI, on the island of Svalbard (designated Station AS72 of the IMS).

the purposes of signal detection, we exploit waveform similarity at both local and regional distances to provide the best possible constraints on the location of events. Waveform similarity alone was demonstrated by *Menke* (2001) to constrain the location of seismic events using a simple model by which the correlation coefficient between the signals from two events decreased exponentially with event separation. More recently, *Massa et al.* (2006) have devised a fully-automatic quasi-real-time algorithm for locating events by cross-correlation using only a single seismic station. *Shearer* (1997), among others, demonstrates how event location estimates can be improved dramatically by the combined use of absolute arrival time readings with higher accuracy cross-correlation relative time measurements. The double difference procedures (see *Waldhauser and Ellsworth*, 2000; *Waldhauser*, 2001) apply such measurements taken over potentially enormous data sets to invert for multiple hypocenter estimates simultaneously. The current state of multiple-event earthquake location methods is reviewed by *Richards et al.* (2006).

A sequence of earthquakes in the Rana region of Northern Norway during 2005 has provided an excellent opportunity to study the extent to which small seismic events can be detected by signal matching at a distant station as a function of event magnitude and distance from a master event. Fig. 1 shows the location of the largest event in the sequence in relation to the stations of the Norwegian National Seismic Network (NNSN), operated by the University of Bergen, and also to the Fennoscandian IMS seismic arrays NORSAR (PS27), ARCES (PS28), Hagfors (AS101) and FINES (PS17). The NNSN exists primarily for the investigation of earthquakes within Norwegian territory whereas the arrays were primarily installed to detect the signals from distant underground nuclear tests. Regional events are located automatically by the network of arrays by a judicious association of detected phases (*Ringdal and Kværna*, 1989) and *Kennett* (2002) illustrates how a seismic event very close to the sequence studied here is located to an acceptable accuracy by the network of arrays despite the absence of any very nearby stations. The earthquake sequence is particularly interesting for our purposes since the largest of the events (approximate magnitude 3.5) was well recorded by stations at quite large distances from the source, whereas many of the smaller events were not detected at the array stations by traditional energy detectors. The stations of the NNSN confirm the presence and timing of the smaller events and allow far better constraints to be applied to the locations of these earthquakes than would otherwise be possible.

Section 2 presents an overview of the events in the Rana region during 2005 which were observed at NORSAR and the other IMS arrays at distances exceeding 600 km. Given the observed waveform similarity of some of these events, we describe the development of a matched filter detector aimed at detecting occurrences of weaker events in this region. We discuss the limited number of detections obtained during 2005 using the large aperture NORSAR array and address how the validity of some of these can be supported by repeating the procedure on different array stations and thus providing independent observations.

Section 3 provides an overview of the closest stations of the NNSN to the target region and demonstrate the improvement in location estimates which can be achieved using recordings from the closest stations. We display all the waveforms available which correspond to the times of the matched filter detections at NORSAR and conclude that almost all of the NORSAR detections correspond to real events in the Rana region.

Section 4 addresses the extent to which we are able to constrain the relative locations of the detected events using recordings from local and from regional distances.

Table 1
Events exceeding magnitude 2.0 in the Rana region during 2005 with NORSAR analyst locations based only upon phase readings from the IMS arrays displayed in Fig. 1

Event ID	Date	Origin time (GMT)	Latitude	Longitude	Magnitude
7872	28 April	2005-118:15.08.56.31	66.3387	13.8208	2.51
7875	1 May	2005-121:07.27.30.52	66.2052	13.4615	2.41
8033	24 June	2005-175:04.25.39.87	66.3780	13.6786	3.45
8368	13 October	2005-286:14.08.38.88	66.3674	13.4287	3.09
8559	15 December	2005-349:16.47.12.31	66.3384	13.8664	3.03

The origin time is given in the format *yyyy-ddd:hh.mm.ss.msc* where *ddd* is the julian day. Depth is fixed to zero for all locations and magnitude estimates are provided by the GBF algorithm (*Ringdal and Kværna*, 1989).

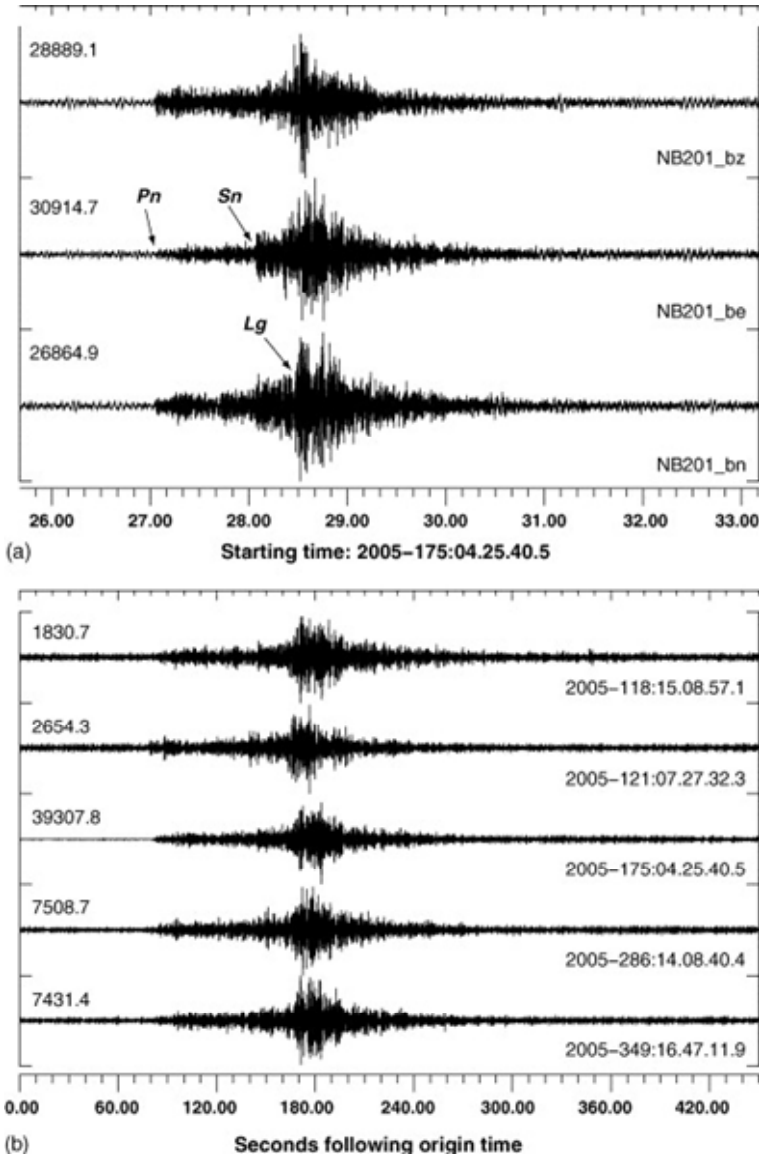

Fig. 2. Recordings at the NORSAR array of the five events listed in Table 1. Panel (a) shows unfiltered waveforms for event 8033 on the vertical, east-west and north-south components of the broadband NB201 three-component instrument. Panel (b) shows short period vertical waveforms, band-pass-filtered between 2.0 and 5.0 Hz, for all five events at the central NB200 seismometer. Maximum amplitudes are given in the upper left hand corner for each trace.

Finally, in Section 5, we summarize the detection and measurement of systematic timing errors on single sensors of the arrays using inconsistencies in the measurements of times of maximum cross-correlation.

2. A sequence of earthquakes in Northern Norway: detections at the Nordic IMS array stations

The Rana region in Northern Norway is known for its relatively high constant seismicity (see, for example, *Hicks et al.*, 2000 and is also the site of one of the largest known earthquakes in Fennoscandia in recent history (M_S 5.8-6.2 on 31 August 1819). Many regions on the north Norwegian coastline have been the sites of earthquake swarms; for example, *Meløy* between 1978 and 1979 (*Bungum et al.*, 1979) and Steigen in 1992 (*Atakan et al.*, 1994). Five events in this region during 2005 were large enough to be detected by more than one of the IMS array stations displayed in Fig. 1; these are listed in Table 1. A few more events were detected by the ARCES array alone but, with estimated magnitudes well below 2.0, they were not included in the reviewed event bulletin. Waveforms from the events listed in Table 1 recorded at the NORSAR array are displayed in

Table 2
Mean normalised correlation coefficients for 180.0 s long data segments averaged over all 42 short-period vertical channels of the NORSAR array for all event pairs from the five events listed in Table 1

Day of event	Day of event				
	28 April	1 May	24 June	13 October	15 December
28 April	1.0	0.0292	0.7878	0.0267	0.6170
1 May	0.0264	1.0	0.0241	0.0234	0.0263
24 June	0.7249	0.0189	1.0	0.0233	0.7483
13 October	0.0205	0.0215	0.0246	1.0	0.0237
15 December	0.4689	0.0251	0.6569	0.0194	1.0

Diagonal elements are all trivially equal to unity. Entries in the table above and below the diagonal are obtained in the 2.0-5.0 Hz and 3.0-8.0 Hz frequency bands, respectively.

Fig. 2. Since the events are almost due North of the array, the *be* and *bn* components of the broadband seismograms resemble the transverse and radial rotations respectively, apart from a difference in sign. The *Sn* arrival is very much clearer on the horizontal components than the vertical components.

Fig. 2 indicates that the signals recorded at NORSAR from these events have a good signal to noise ratio (SNR) in the frequency bands examined for at least 3 min following the initial P-arrival. To quantify the degree of waveform similarity for each pair of events, we calculate a fully-normalised correlation coefficient by sliding a waveform template from the first event over a selected time-window for the second event and recording the maximum correlation coefficient obtained. We in fact calculate an "array correlation coefficient" trace (cf. *Gibbons and Ringdal*, 2006) which is a beam whereby the normalised correlation coefficient traces for the individual sites are delayed and averaged according to a set of imposed time-delays. Due to the large inter-site distances on the NORSAR array, the definition of the data-windows in the waveform template is not trivial. For the definition of these templates, we define for each event a reference time t_R which, for simplicity, is an estimate of the event's origin time. For a fixed estimate of the event origin location (latitude, longitude and depth), we define the start of the time window for site i as $t_R + \tau_i$ where τ_i is the travel time of a specified seismic phase between source and receiver for the most appropriate one-dimensional velocity model (in this case, the Fennoscandian model, *Mykkeltveit and Ringdal*, 1981). For these templates, the master waveform for each site consists of 180.0 s of data beginning at the predicted *Pn*-arrival for the given master event. Whilst the time-windows for each channel (τ_i are in this case complicated functions of the master event origin location and chosen velocity model, provided that the same time-delays are applied by the detector as were used in the template definition, all subsequent correlation detection times, t_D, are related only to the reference time, t_R. A slightly different set of τ_i (for example, corresponding to a different location estimate or a different velocity model) will result in a different correlation coefficient but, providing that the templates contain largely the same data, the maximum correlation coefficient should occur at the same time and hence result in the same detection time, t_D. If the time of the maximum correlation coefficient is not stable to small changes in the signal template specification, it is a sure indication that the observed waveform similarity is spurious or insignificant.

For each pair of events from the selected five, an array correlation coefficient was calculated in two different frequency bands; these are listed in Table 2. Three of the events considered (the events of 28 April, 24 June and 15 December) indicate a very high degree of waveform similarity with correlation coefficients exceeding a relatively high value of 0.46 in both frequency bands for all event pairs. The events of 1 May 2005 and 13 October 2005, did not display a significant degree of waveform similarity with any of the other events with maximum correlation coefficients typical of those obtained between randomly selected data segments of the same length and bandpass filtering. For the given event pairs, the Cross-correlation coefficient obtained in the 2.0-5.0 Hz frequency band is always greater than that obtained in the 3.0-8.0 Hz frequency band (i.e. the coefficients above the diagonal in Table 2 are greater than the corresponding values reflected in the diagonal). Although the SNR is greater at the higher frequencies, the wavelengths involved are shorter and the waveforms are hence more susceptible to distance between hypocenters and consequently smaller scale path heterogeneities. The events in Table 1

displaying the greatest degree of waveform similarity are the events on 28 April and 24 June. Despite over an order of magnitude difference in waveform amplitudes, the correlation coefficient exceeds 0.7 even for a 3-min long data segment filtered between 3.0 and 8.0 Hz. The correlation coefficients obtained between the largest event (24 June) and the smaller events (28 April and 15 December) are greater than the correlation coefficient obtained between the two smaller events. This may be indicative of the relative locations of the three events or the result of the larger magnitude of the 24 June event. Waveform data from closer stations would be needed to address this.

A waveform correlation detector as described by *Gibbons and Ringdal* (2006) was prepared using the waveforms from the 24 June event as a signal template with the purpose of detecting seismic disturbances in the immediate vicinity of these earthquakes, too small to be detected by the IMS arrays using traditional energy detectors. Such disturbances could be either aftershocks immediately related to the largest events or nearby tremors at other times. It is clear from examining the correlation coefficients in Table 2 that each of the events 28 April, 24 June and 15 December would be detected by such a system given the ratio between the maximum correlation coefficient obtained and the background values. A waveform template was defined as above, related to predicted *Pn*-arrivals at each site, but this time using a data segment of length 120.0 s, bandpass filtered between 2.0 and 8.0 Hz. The detector was run on continuous data from the NORSAR array for the whole of the calendar year 2005.

As for any detector, we need to declare the circumstances under which a detection is defined. For the correlation detector, we seek significant values of the normalised correlation coefficient or, in the array situation, the array correlation beam. *Gibbons and Ringdal* (2006) defined a scaled correlation coefficient which, analogously to an SNR, indicates the ratio between the correlation coefficient at a given time and the background level at surrounding times. (A similar quantity has subsequently been demonstrated by *Schaff and Waldhauser*, 2006, to provide a very stable detection statistic for correlation detectors on three-component stations.) For the current investigation, the values of the (unscaled) correlation beam were examined for many different data segments, of which three are displayed in Fig. 3. The uppermost panels in Fig. 3 correspond to a data segment in which no signals are observed. The correlation coefficient for a single channel does not exceed ± 0.14 and the zero-delay stacking over the 42 sites of the NORSAR array reduces the variability of the correlation beam to within ± 0.02 over the 10-min interval. The linearity of the quantile-quantile plot (upper right panel in Fig. 3) indicates that the values of the correlation beam are almost perfectly normally distributed for this interval. The normal distribution with this standard deviation appears to be quite typical for data segments without detections. The presence of any seismic signal appears to complicate matters and an example featuring a completely unrelated regional signal is displayed in the central panels of Fig. 3. The foreign signal leads to a modulation of the correlation coefficient traces and the quantile-quantile plot indicates a departure from the normal distribution and an increase in the extreme values observed. Similar plots were observed for large numbers of different signals; the highest values of the correlation beam and the greatest departures from a normal distribution observed were for regional signals from the Rana region. The values of the correlation beam obtained using this template at the time of event 8368 in Table 1 ranged from -0.269 to 0.252.

For all the data segments examined, with the exception of the times of events known to correlate well with the waveform template (cf. Table 2), the correlation beam was never observed to exceed a value of 0.03. The signal and correlation coefficients corresponding to the time of the 28 April 2005, earthquake are displayed in the lowermost panels of Fig. 3. The difference between the single channel and full-array correlation coefficient traces is very clear with several clear peaks observed in the array beam which do not rise above the background levels in the single channel case. The nominal threshold value of 0.03 is exceeded at the times indicated by A, B, C, and D on the lowermost trace. On closer inspection, the correlation peak at time C actually consists of two distinct maxima separated by approximately 2.5 s. Whilst we expect 0.03 to constitute a robust detection threshold, we report initially all occasions on which a value of 0.025 is exceeded and, in addition, all occasions on which the scaled correlation coefficient (as defined by *Gibbons and Ringdal*,

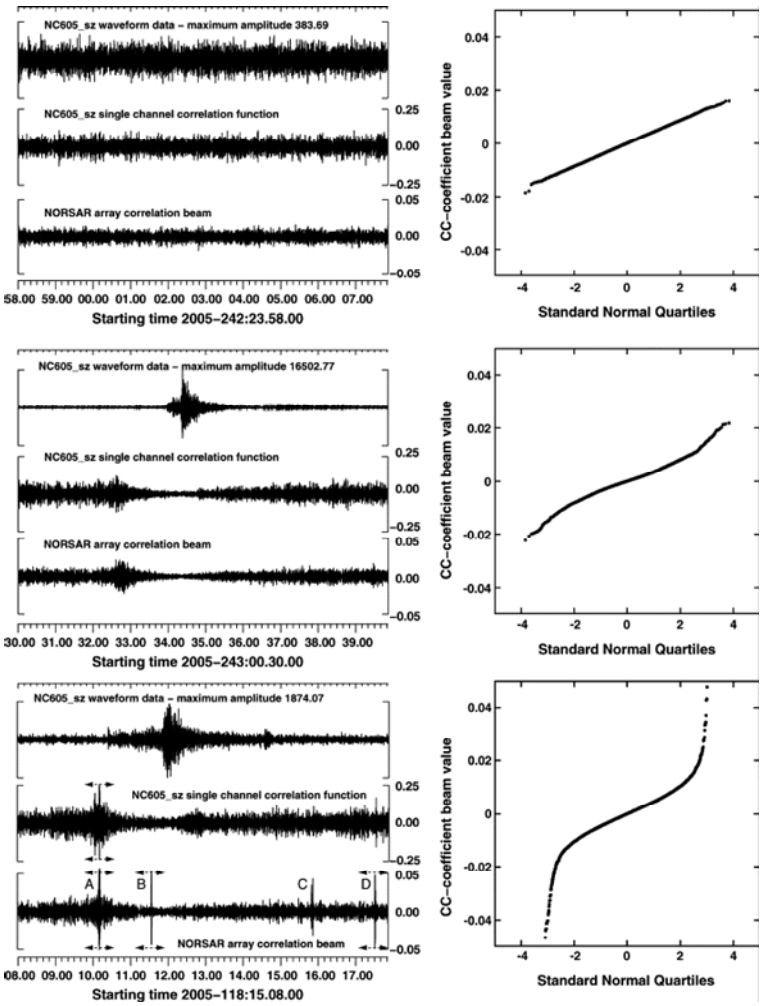

Fig. 3. Selection of a detection threshold for a correlation detector on the NORSAR array where the template consists of 120.0 s long data segments of waveforms, bandpass filtered between 2.0 and 8.0 Hz, corresponding to the event with ID 8033 in Table 1. The left panel in each row displays a 10-min long filtered data segment on a single channel together with the corresponding correlation coefficient channel and the correlation beam. The right panel in each row shows the values of the correlation beam reordered and plotted against the standard normal quantiles. The correlation traces in the bottom row are clipped as indicated.

2006) exceeds a value 6.0. On each occasion on which a local maximum is identified in the correlation beam, a detection reduction rule prevents any subsequent detection being made within 3.0 s of this time.

Fig. 4 displays the fully normalised array coefficient for each of the 554 occasions during 2005 for which these provisional detection criteria were met. The value unity is obtained exactly once: for the time interval corresponding to the master waveform template. It is clear from the distribution of points in Fig. 4 that any reduction in the detection threshold below the provisional value of 0.03 suggested by examination of the quantile-quantile plots in Fig. 3 would result in a large increase in the number of detections. Since tests involving unrelated signals frequently resulted in coefficients exceeding 0.020, it is clear that a robust threshold must be set higher. On the basis of Figs. 3 and 4, it was deemed that 0.03 appeared to constitute a sensible threshold and all provisional detections where the correlation beam did not exceed 0.03 were discarded. This threshold was exceeded on 32 occasions during 2005, almost none of which corresponded to times when a signal detectable by traditional energy detectors was observed on the NORSAR array. These instances are listed in Table 3.

The next task is to check which of the correlation detections listed in Table 3 correspond to verifiable events in the Rana region. Detections 7, 23 and 30 clearly correspond to the 28 April, 24 June and 15 December events in Table 1. Other detections have far more marginal correlation coefficients and may correspond to coincidental similarity with segments of noise or signals incident from

Table 3
NORSAR correlation detections (see Fig. 4) for which the array correlation coefficient exceeded 0.03

Det.	Date	Julian time	C.C. coefficient	Scaling factor	Mag.
1	25 January	025:16.47.29.719	0.0330	0.000037	-0.93
2	6 February	037:02.13.07.446	0.0740	0.000770	0.39
3	19 February	050:04.03.00.086	0.1411	0.001730	0.74
4	4 March	063:10.32.20.833	0.3796	0.007940	1.40
5	6 April	096:10.54.57.970	0.0432	0.000543	0.23
6	28 April	118:10.48.42.936	0.0662	0.000901	0.45
7	28 April	118:15.08.57.788	0.7970	0.044560	2.15
8	28 April	118:15.10.21.033	0.0854	0.004700	1.17
9	28 April	118:15.14.38.837	0.0487	0.000348	0.04
10	28 April	118:15.16.18.097	0.1267	0.001410	0.65
11	28 April	118:15.50.02.263	0.0636	0.000672	0.33
12	30 April	120:12.41.24.221	0.0682	0.000687	0.34
13	15 May	135:03.31.10.775	0.0602	0.000461	0.16
14	16 May	136:07.00.16.105	0.0534	0.000562	0.25
15	19 May	139:03.58.24.572	0.0859	0.000795	0.40
16	21 May	141:11.28.53.963	0.0493	0.000670	0.33
17	2 June	153:14.07.49.892	0.1846	0.002650	0.92
18	10 June	161:15.39.30.817	0.2854	0.004390	1.14
19	10 June	161:16.25.34.695	0.1486	0.002140	0.83
20	10 June	161:16.39.01.043	0.0435	0.000481	0.18
21	10 June	161:17.46.26.336	0.0309	0.000250	-0.10
22	17 June	168:00.50.55.884	0.0664	0.000645	0.31
23	24 June	175:04.25.41.000	1.0000	1.000000	3.50
24	24 June	175:05.02.16.254	0.1741	0.002790	0.95
25	5 September	248:04.58.22.973	0.4419	0.007200	1.36
26	12 September	255:23.49.03.892	0.0774	0.000747	0.37
27	24 September	267:09.56.29.013	0.0354	0.000360	0.06
28	19 October	292:19.40.56.155	0.1355	0.001330	0.62
29	14 December	348:05.53.06.775	0.0577	0.000663	0.32
30	15 December	349:16.47.13.008	0.7363	0.165670	2.72
31	15 December	349:16.47.57.783	0.0497	0.010390	1.52
32	31 December	365:09.54.11.126	0.0443	0.000422	0.13

C.C. coefficient is the fully-normalised array correlation coefficient and the scaling factor, α, is the scalar multiple of the master waveform which minimises the residual when the detected waveform is subtracted (see *Gibbons and Ringdal*, 2006). The subsequent magnitude estimate is given by $M = \log_{10}(\alpha) + 3.5$. The reference time, t_R, used is 2005-175:04.25.41.000.

other source regions. In addition to the low values of the correlation coefficients, the corresponding scaling factors (denoted α in *Gibbons and Ringdal*, 2006) are also very low for all the remaining detections. To make these numbers more tangible, we assign a magnitude 3.5 to the master event and estimate crudely that a scaling factor of α will correspond to a magnitude $M = \log_{10}(\alpha) + 3.5$. The magnitude estimates of 2.16 and 2.73 for the 28 April and 15 December events are slightly lower than (albeit of the same order as) the respective GBF magnitude estimates of 2.51 and 3.03. The lower magnitude estimates are likely to be the result of waveform dissimilarity between the events. This estimate assumes that the residual between the scaled waveform template and the detected waveform is entirely random, and this will not be the case when the signals are deterministically different.

A first approach to verifying the presence of events for each of these detections is to apply a similar procedure for each of the other IMS arrays displayed in Fig. 1. Assuming that two events are co-located, and produce similar waveforms, then the time separating the corresponding patterns in the wavetrains will be identical for all stations (this is exactly the principle on which the beamforming of the correlation coefficient channels works). Therefore, assuming also that the SNR is sufficient for a detection, all stations should indicate an identical detection time (relative to the reference time for the master event). An analogous correlation detector was run over short time-windows surrounding each of the NORSAR detections in Table 3 for each of the remaining Nordic IMS array stations (ARCES, FINES, Hagfors and SPITS). Unlike the detection procedure carried out using the NORSAR array, which correlated the waveform template against every possible data segment recorded during the year 2005, the detectors on the regional arrays have not yet been run continuously. A detection was declared for the regional arrays if and only if the maximum correlation coefficient attained exceeded the standard deviation for the whole time interval by a factor of 5 or more.

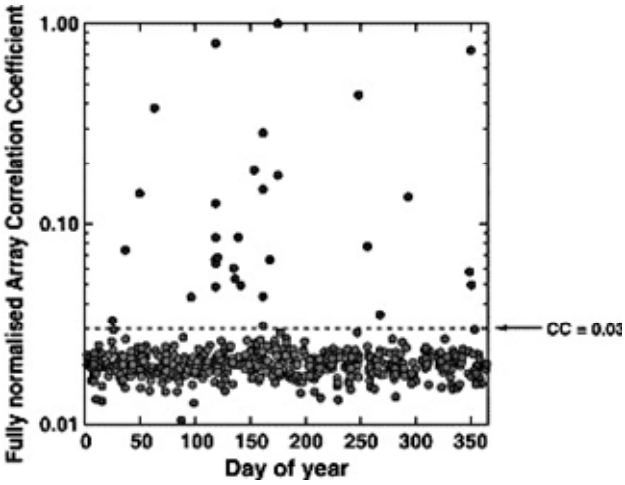

Fig. 4. Preliminary detections between 1 January 2005 and 31 December 2005 for a matched filter detector on the NORSAR array where the template consists of 120.0 s long data segments of waveforms, bandpass filtered between 2.0 and 8.0 Hz, corresponding to the event with ID 8033 in Table 1. Each detection was triggered by either an array correlation coefficient exceeding 0.025 or a scaled array coefficient exceeding 6.0.

Table 4 displays the corresponding detection times for each of the arrays indicated for all of the 32 detections made on the NORSAR array. Despite the table offering no information other than a time of maximum correlation (or an indication that no detection was made), many remarkable observations are possible. The first is that the essentially equidistant ARCES array (25 sites within an aperture of approximately 3 km) reports a detection within a small fraction of a second for all but two of the correlation detections made by the NORSAR array. The first of these detections (on 25 January) was not detected by any of the other array stations and the arrival of a strong teleseismic P-phase within the 2 min following this time indicates a high probability that this marginal correlation is a false alarm. Nothing further can be inferred about an event on 6 April 2005 (detection number 5) since ARCES suffered a power outage at this time and any event, if present, was too weak to be detected by any of the more distant arrays. Given that these 32 detections are the only occasions on which this matched filter detector triggered within the space of a calendar year, and that 30 of these are matched to within no more than 0.15 s by entirely independent array observations from almost the opposite direction indicates that the likelihood that this detection list contains a large number of false alarms is very small.

The second major observation from Table 4 is the small amount by which the detection reference times differ. Almost all the values quoted are zero to within at most a few samples (the NORSAR, ARCES and FINES arrays are sampled at 40 Hz whilst SPITS and HFS are sampled at 80 Hz). For a sampling interval of 0.025 s, the four decimal places quoted in Table 4 appear excessive given that this precision is the combination of both FIR-filter resampling of the waveforms and a spline interpolation of the correlation coefficient traces. However, an accuracy of 0.001 s is quite reasonable for such cross-correlation calculations (see, for example, *Poupinet et al.*, 1984) which means that the additional decimal places are required simply to eliminate the effect of numerical round-off in arithmetic. Three factors contribute to a non-zero difference between detection times at different stations:

(1) a distance between the hypocenters of two subsequent seismic events will lead to changes in the relative travel times to different receiver sites;
(2) waveform dissimilarity (be it the result of differences in the source, the path, or background noise in the case of a low signal-to-noise ratio at the receiver) will lead to correlation coefficient traces which may not result in a maximum value at the expected time;
(3) systematic timing problems at the receiver.

Aside from single-site aberrations, which are discussed further in Section 5, only one systematic timing error is known to exist in the array data used in this paper. The Spitsbergen array, between 3 August 2005 and 31 December 2005, put a time stamp on data which was 1 s ahead of Universal Time; this was the result of a manufacturing error, announced and documented by the supplier of the instruments, to compensate for the leap second on 31 December 2005. If data from this array had not been duly corrected prior to the analysis, the entry for SPI for detection 30 would read -1.0390.

The non-zero entries in Table 4 are therefore presumably due to a combination of the first two factors stated above. There are very few values which are clearly anomalous, δt at HFS for detection 9 being an obvious exception. The Hagfors array in fact shows the smallest deviations from the detection times at the NORSAR array. Being the array which is geographically closest to the NORSAR array, the small δt at HFS suggest that

Table 4
A waveform correlation detector was run on each of the Nordic IMS array stations for short time-windows surrounding each of the detections listed in Table 3

Det.	t_0: NORSAR	δt: ARC	δt: rARC	δt: HFS	δt: FIN	δt: SPI
1	025:16.47.29.71983	-	-	-	-	-
2	037:02.13.07.44567	0.0809	0.0791	-0.0034	0.0053	-
3	050:04.03.00.08567	0.1421	0.1421	0.0116	0.0919	-
4	063:10.32.20.83350	0.0635	0.0639	0.0044	0.0411	-
5	096:10.54.57.96950	No data	No data	-	-	-
6	118:10.48.42.93517	0.0490	0.0490	-0.0060	-	-
7	118:15.08.57.78750	0.0325	0.0333	0.0046	-	0.0242
8	118:15.10.21.03167	0.0051	0.0063	0.0010	-	-
9	118:15.14.38.83600	0.0316	0.0294	0.4601	-	-
10	118:15.16.18.09733	0.0615	0.0623	0.0062	-	-
11	118:15.50.02.26317	0.0608	0.0594	0.0093	-	-
12	120:12.41.24.22050	0.0401	0.0389	0.0045	-	-
13	135:03.31.10.77600	0.0250	0.0084	-	-	-
14	136:07.00.16.10533	-0.0099	-0.0133	-	-	-
15	139:03.58.24.57183	0.0304	0.0326	0.0101	-	-
16	141:11.28.53.96217	0.0062	0.0048	-	-	-
17	153:14.07.49.89133	0.0317	0.0325	0.0041	0.0219	-
18	161:15.39.30.81667	-0.0145	-0.0129	0.0009	-0.0081	-
19	161:16.25.34.69450	-0.0217	-0.0203	-0.0002	-0.0129	-
20	161:16.39.01.04267	-0.0303	-0.0279	-	-	-
21	161:17.46.26.33400	-0.0242	-	-	-	-
22	168:00.50.55.88450	0.0231	0.0225	-	0.0153	-
23	175:04.25.41.00000	0.0000	0.0000	0.0000	0.0000	0.0000
24	175:05.02.16.25400	-0.0314	-0.0308	-0.0001	-0.0274	-
25	248:04.58.22.97267	-0.0243	-0.0229	-0.0015	-0.0189	-
26	255:23.49.03.89300	-0.0500	-0.0466	-0.0045	-0.0172	-
27	267:09.56.29.01283	-0.0674	-	-	-	-
28	292:19.40.56.15483	0.0224	0.0248	-0.0008	-	-
29	348:05.53.06.77517	-0.0518	-0.0514	-0.0165	-	-
30	349:16.47.13.00883	-0.0582	-0.0570	-0.0017	-0.0344	-0.0390
31	349:16.47.57.78367	0.0049	-0.0123	-	-	-
32	365:09.54.11.12583	-0.2224	-0.2196	-	-	-

In each case, the template signal consisted of 120.0 s of data, bandpass filtered between 2.0 and 8.0 Hz, starting with the first predicted phase arrival where the event reference time, t_R, is set to 2005-175:04.25.41.000. All waveforms were resampled to 200 Hz and a spline interpolation scheme was used to find the time of the cross-correlation beam maximum. The first time provided is the corresponding reference time, t_0 for each event according to correlation on the NORSAR array. The reference times for the listed arrays are given by $t_0 + \delta t$. rARC denotes a reduced ARCES array consisting of only the innermost nine elements. A dash indicates non-detection.

the δt are dominated by varying locations of the events. The close correspondence between the maximum correlation times at the full ARCES array and the nine element subset (denoted rARC) suggests that waveform dissimilarity does not contribute greatly to the changes in time measurements; were waveform dissimilarity significant, the additional correlation coefficient channels added when the whole array is considered would probably have a far greater effect on the estimated time of maximum correlation. The δt for the regional arrays relative to NORSAR in the first half of the year appear to be largely positive and those towards the latter part of the year appear to be largely negative. This could indicate a systematic shift (for example drift along a fault) of hypocenter locations. The relative locations of events is discussed in Section 4.

A further piece of information provided by Table 4 relates to the detectability of the various events by the different arrays. The full and continuous detection process was only run on the NORSAR array and we assume that the 32 detections shown are the only ones obtainable in this period. (It is of course possible that a continuous detector run on the ARCES array would detect further events not picked up by NORSAR.) As previously stated, the full ARCES array resulted in detections which matched all but two of the NORSAR detections. The reduced ARCES array fails to pick up a further four of these detections. The reduced configuration, consisting of the central element and the eight instruments contained in the innermost A and B rings, was purposefully chosen since this design most closely matches the standard by which most new array installations are being designed. It also provides a closer comparison with the Hagfors array, which exhibits a similar, albeit slightly poorer, detection capability. This could be due to the slightly greater distance from the source, different noise conditions at the different arrays, or differences in signal attenua-

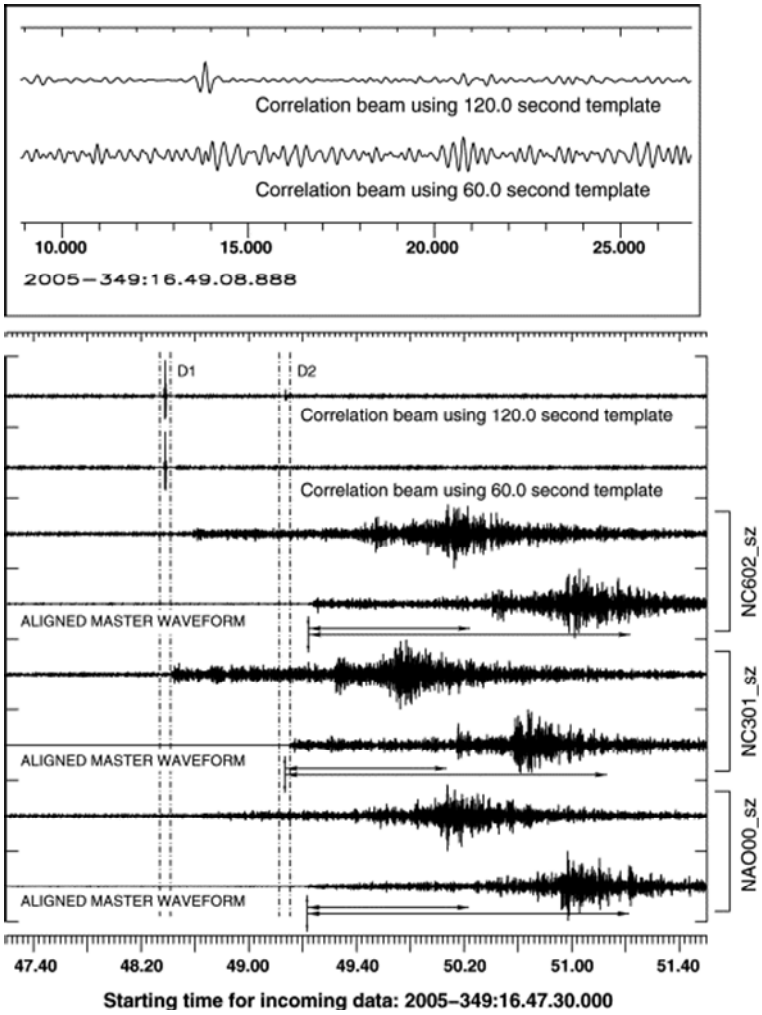

Fig. 5. Detection using the NORSAR array of a presumed aftershock to the main event on 15 December 2005, using the 24 June main event signal as a template. D1 and D2 correspond to detections 30 and 31 in Table 3. Incoming data is shown for three channels as indicated together with the corresponding segments from the master event, aligned according to the time of detection D2. Note how the master waveform segments are staggered according to the *Pn* arrivals. The correlation coefficient beams are displayed for the cases of 60.0 and 120.0 s long waveform templates and it is clear (see inset panel for details) that the very marginal detection 31 (D2) is not made when only the shorter data segment is used. The actual segments of data corresponding to the two window lengths are indicated by arrows below the master waveform segments.

tion along the propagation paths.

The FINES array is at a slightly greater distance again than the Hagfors array and, whilst consisting of 16 sites as opposed to the nine at Hagfors, matches significantly fewer of the NORSAR detections. Nevertheless, 14 out of a possible 32 detections are matched and each with a very small time-residual. The nine-site Spitsbergen array at a distance of over 1300 km is only able to detect the two largest events of 28 April and 15 December using the signal from the 24 June event as a master waveform template. Whilst not assisting our search for further events from this region, this is an encouraging result in the field of CTBT monitoring since the signal resulting from this magnitude 3.5 event registered a fairly low SNR at the SPITS array and yet using a matched field detector with this weak signal is nevertheless able to detect two events of up to an order of magnitude smaller.

The final comment to be made about Tables 3 and 4 is that several of the detections occur in quick succession of each other. The lowermost panel of Fig. 3 indicates four peaks within a period of 10 min. (Detections 7-10 in Table 3 correspond to the letters A, B, C and D in Fig. 3; only one detection is registered for C because of the detection reduction rule.) In the cases of the detections on, for example, 10 June and 24 June there is approximately an hour separating each of the correlation detections. Assuming that each of these detections does actually correspond to a real event, the fact that each of the detections is distinct (i.e. the time separating the detections is far longer than

the length of the waveform template) means that each must correspond to a distinct event. The sequences of detections on 28 April and 15 December are more difficult to judge without additional information; only 42 s separate detections 30 and 31 (on 15 December) and so the second detection comes during the wavetrain corresponding to the first detection. A multiple correlation detection can be caused if the waveform template is contaminated with the signal from an aftershock. However, in this situation, all subsequent detections would come in multiples of two (with the same time-separation for every event at every station) which is clearly not the case. The fact that the different arrays produce detections with self-consistent times essentially rules out self-similarity of coda waves as a cause of the multiple detections, as does the fact that the same pattern is not observed for each event. We conclude that the multiple detections are likely to be the result of distinct seismic events.

Fig. 5 shows the sequence of detections occurring on 15 December 2005. We demonstrate here that the weakest of these detections (detection 31 in Table 3) is not possible when a data segment of only 1 min, beginning at the *Pn* arrival, is used. Assuming that this secondary detection does indeed correspond to a small aftershock, the timing is such that a minute of P-coda from the aftershock arrives at the NORSAR array at the same time as the greatest amplitudes in the regional wavetrain: the *Sn* and *Lg* phases. A corollary is that, when selecting data segments for correlation detectors, it is more important to select a section of the signal with the largest amplitude than a segment containing the start of the wavetrain.

3. Observations of events from stations of the Norwegian National Seismic Network (NNSN)

Fig. 6 indicates the locations of the five NNSN stations which are closest to the Rana sequence, together with two location estimates for the 24 June main event. The white circle indicates the location estimate obtained using only the Fennoscandian IMS arrays. The location estimate indicated by the star (66.409°N, 13.324°E with depth 13.33 km) was obtained using the HYPOSAT program (*Schweitzer*, 2001a) using only P- and S-picks, together with polarisation based P-phase azimuth and slowness estimates, from the waveforms displayed. The Stokkvågen station, STOK, is situated to the South-West of this sequence and has been a part of the NNSN since the summer of 2003. Fig. 6 shows how the S-arrival at STOK is over an order of magnitude larger than the P-arrival on all components. This is not the case for the temporary STOK1 Station to the north-west of the events; here, the P-amplitude is of the same order as S- on the vertical and radial components.

Unlike the IMS array stations, which record and archive continuous data, most of the NNSN stations are triggered and it is often not possible to inspect data for a requested time-interval in the past. However, as displayed in Fig. 7, the STOK station did archive data for the time-intervals corresponding to almost all of the 32 correlation detections at NORSAR. With the waveforms aligned according to greatest correlation coefficient for a window following the S-arrival, these signals appear almost identical at a glance; they are primarily differentiated by the large differences in amplitudes. Over three orders of magnitude separate the amplitudes for detections 21 and 23 which, given the waveform similarity, allows us to conclude an approximate three orders of magnitude difference in the corresponding event magnitudes. For the P-arrivals to be compared meaningfully, they are displayed in a magnified window in the left panel of Fig. 7. It is clear that the events cannot be precisely co-located since there is a measurable difference in the S-P travel times. Fig. 7 also resolves the issue of the aftershock sequences on 28 April and 15 December, confirming that the detections on the NORSAR array (see Fig. 5) do in fact correspond to distinct events. The weak P-arrival at STOK for detection 31 fails to exceed the coda of the much larger event which occurred 45 s previously. The other detection for which no P-arrival is visible in Fig. 7 is number 9; this is clearly two events occurring a rapid succession of each other and the arrival in the left panel is actually the S-phase from the previous event. These two consecutive events correspond to the two closely-spaced peaks in the NORSAR correlation beam, labelled C in the lowermost panel of Fig. 3.

It should be noted that, for the detections prior to June 2005, the absolute time at the STOK station cannot be relied upon due to a technical problem with the GPS receiver. The fault was repaired and detections including and following 10 June, 2005, are recorded with a correct absolute time.

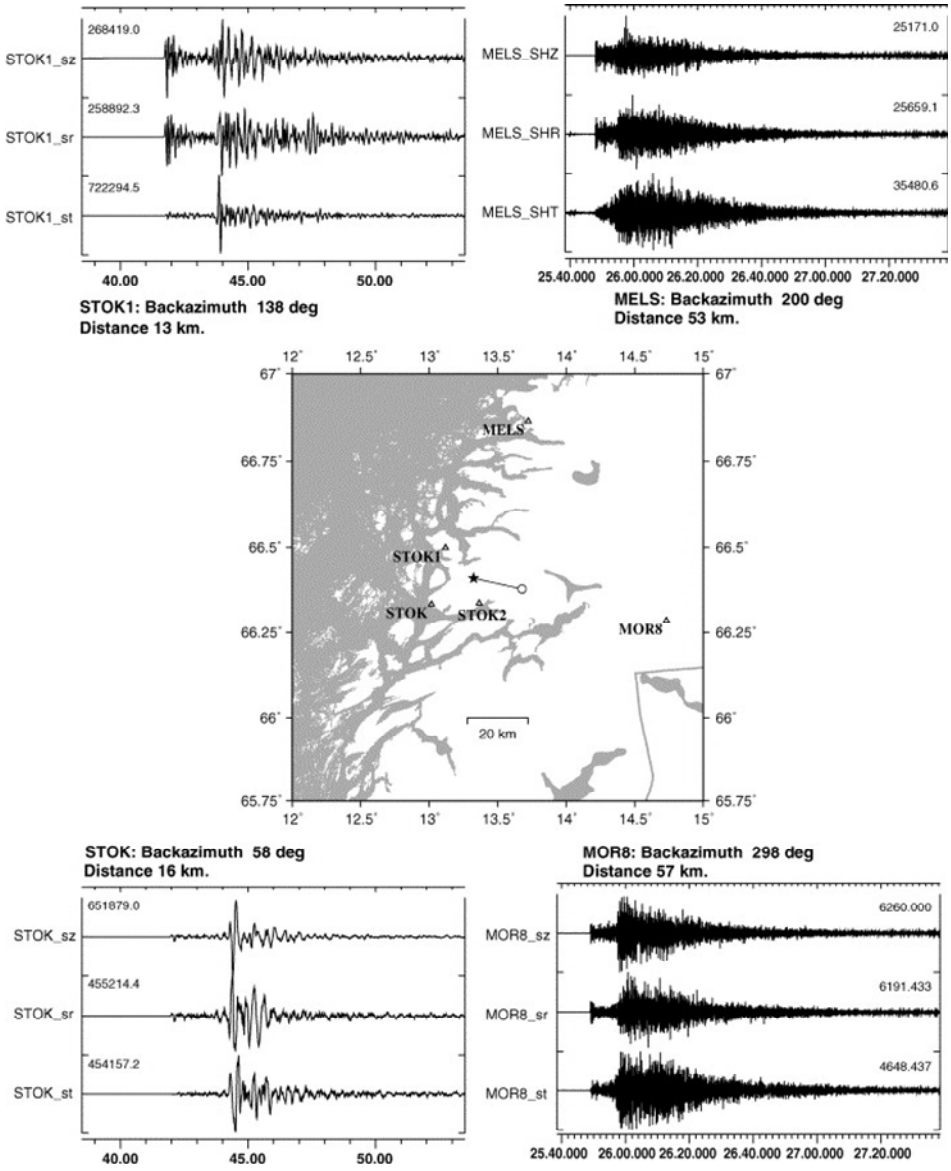

Fig. 6. Location estimates for the 24 Tune 2005, event. The white circle denotes the location indicated in Table 1 and the black star indicates a new estimate based upon P- and S-picks from the four stations displayed: MELS (Meløy), STOK (Stokkvågen), STOK1 (temporary installation) and MOR8 (Mo i Rana). The temporary STOK2 station was not in operation at the time of this event. All waveforms are unfiltered, seismograms all begin at the origin time estimate 2005-175:04.25.38.485, and all horizontal components are rotated according to the backazimuths indicated.

By comparing the time elapsed between events at the IMS arrays and at the STOK station prior to June 2005, we can confirm that the drift never exceeded 0.3 s. However, since this value is very much larger than the uncertainty in the phase picks at the station, only differential S-P times can be used from STOK during this period. It is clear that, for the events displayed in Fig. 7, the S-P time difference is identical to within approximately 0.05 s. Based upon a P-velocity of 6.20 km^{-1} and a $\upsilon_P:\upsilon_S$ ratio of 1.73, this would mean that the hypocentral distance to the STOK station is the same for all events to within approximately 450 m.

The temporary station STOK1 was deployed in June 2005 to the north-west of the cluster and, based upon S-P travel time differences, is probably marginally closer than STOK. Due to technical and logistical difficulties, this station unfortunately recorded only eight of the detected events; the waveforms are displayed in Fig. 8, again aligned according to maximum waveform similarity for the S-arrival. The signals on the horizontal components are very similar for each of the events shown, whereas the vertical component recordings appear to show a progressive change. For this limited number of events, an inspection of the P-arrivals (with alignment according to the S-wave cross-correlation) suggests an even lower range of

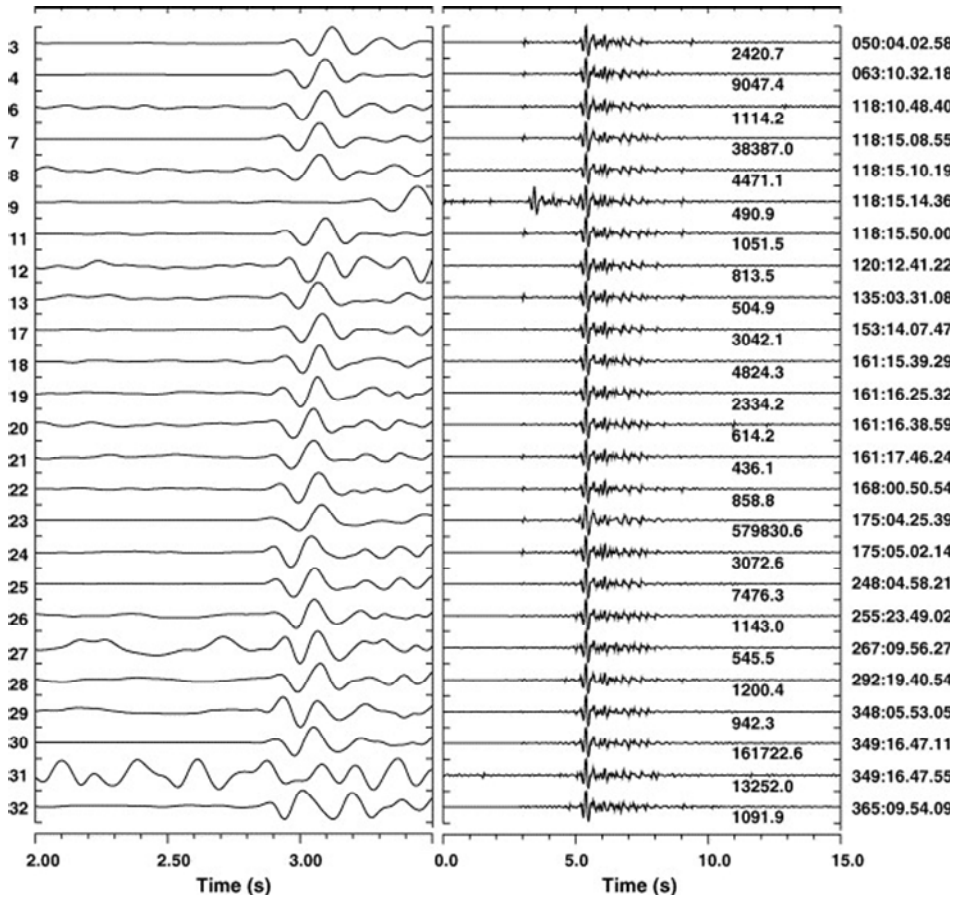

Fig. 7. Waveforms recorded at the STOK station for the times corresponding to the NORSAR correlation detections as listed in Table 3. The right panel displays a 15.0 s long data segment from the short period vertical channel with each waveform aligned to provide maximum correlation with a 2.0 s long window containing the S-arrival for the 24 June main event. The left panel displays a 1.5 s long segment containing the far lower amplitude P-arrival for each event with exactly the same alignment as displayed in the right panel. Observed differences in the P-arrival are indications of S minus P travel time differences for this station. Numbers missing from the left hand side indicate detections in Table 3 for which no STOK data exists. All waveforms are bandpass filtered between 2.0 and 8.0 Hz.

hypocentral separations in the direction of the STOK1 station than was shown for the STOK station.

Given the similarity of the different signals on the horizontal components of the STOK1 station, we can again infer that the amplitude ratios give a reasonable indication of the event magnitudes. Both STOK and STOK1 recorded the main 24 June event and, if we fix the estimated magnitude of this event (we have used 3.5 consistently within this paper), we may calculate magnitude estimates for the other events, *i*, using

$$m_i^S = log_{10}(\alpha_i^S) + 3.5$$

where $\propto$ the ratio for station S between the maximum amplitude of the S-wave for event *i* and the maximum S-wave amplitude for the master event. If this formulation is valid, then the should be essentially independent of the station, *S*. This is confirmed for the limited number of events recorded by both STOK and STOK1 in Fig. 9 where the filled symbols indicate a close correspondence. The amplitude ratios measured at the local stations indicate the smallest of the events detected by the matched filter on the distant NORSAR array were of magnitudes as low as 0.5.

The open symbols in Fig. 9 indicate the relationship between the magnitude estimates obtained from the NORSAR correlation calculations and the magnitude estimates obtained from the STOK recordings. The correspondence is surprisingly good considering the low SNR of the signals at the distant array station, although there is a tendency for the array inversions to underestimate the magnitude, especially for the smaller events. The scaling factors, α, inverted from the correlation calculation (described in detail by *Gibbons and Ringdal*, 2006), are too low by up to half a magnitude unit with the disparity increasing as the SNR de-

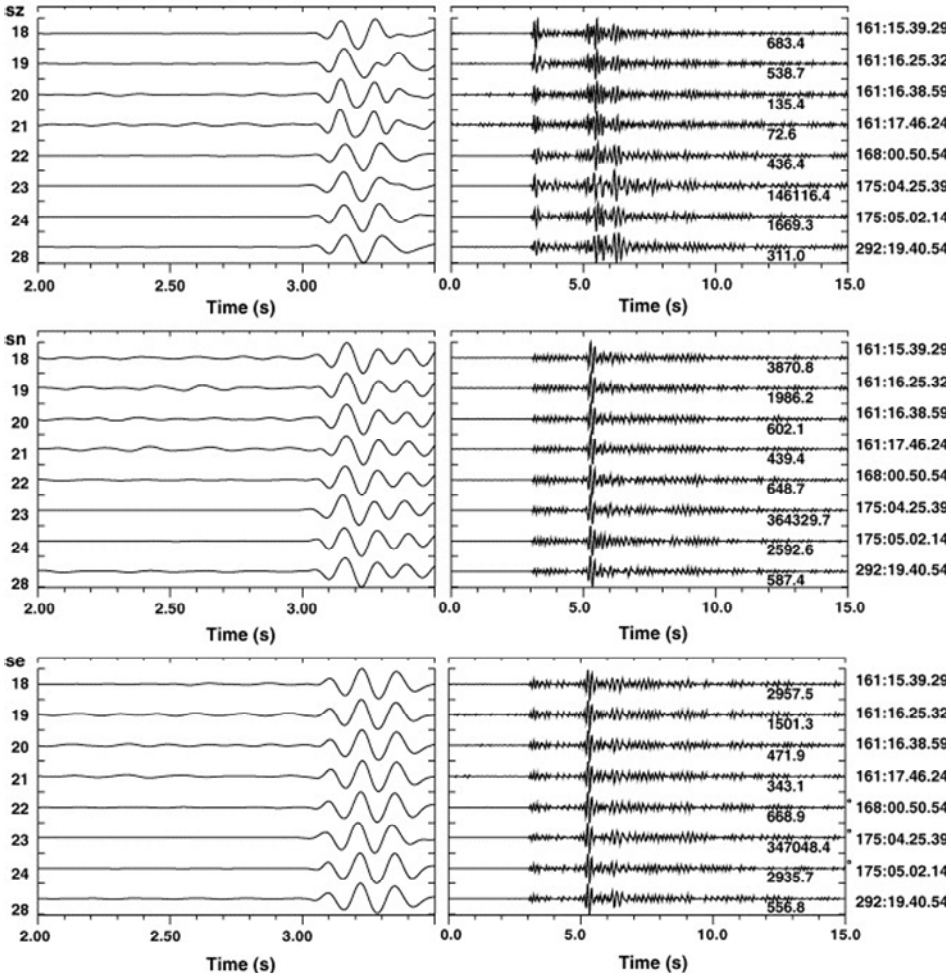

Fig. 8. Waveforms recorded at the STOK1 station for the times corresponding to the NORSAR correlation detections as listed in Table 3. sz, sn and se denote the short period vertical, north-south and east-west components respectively. Alignment in both left and right panels is based upon a maximum correlation with a 3.0 s time-window of the 24 June main event starting at the S-arrival.

creases. The inversion does appear to provide a useful lower bound on the magnitude estimate.

An additional temporary station, STOK2, was also deployed later in the summer of 2005. Based upon S-P travel time differences, this station appears to be the closest of the three. Unfortunately, this is also the station for which we have the fewest recordings with only four of the events in this sequence recorded (see Fig. 10). This is not only unfortunate from the perspective of locating the events, but because the waveforms at this station show the greatest variation from event to event. The 12 September and 24 September events in Fig. 10 (detections 26 and 27 in Table 3) resulted in almost identical waveforms, whereas all other event pairs display significant differences, both in the alignment of features and in the relative size of the P- and S-arrivals. For the STOK and STOK1 stations, the part of the wavetrain which displayed the greatest similarity from event to event was the S-arrival. For the STOK2 station, it is the P-arrival and so the waveforms displayed in Fig. 10 are aligned according to the maximum correlation coefficient at the time of the P-arrival.

Finally, it should be noted that for the detections which were not recorded by the Stokkvågen stations, only detection number 1 in Table 3 was not supported by observations from any of the NNSN stations.

4. The relative location of events detected

Under ideal circumstances, we would have a complete record of every event in the sequence from the local network with which we could calculate accurate relative delay times, for both direct P- and S-waves, and solve for relative locations of the entire sequence simultaneously using the double-difference algorithm as implemented in the hypoDD program (*Waldhauser and Ellsworth*,

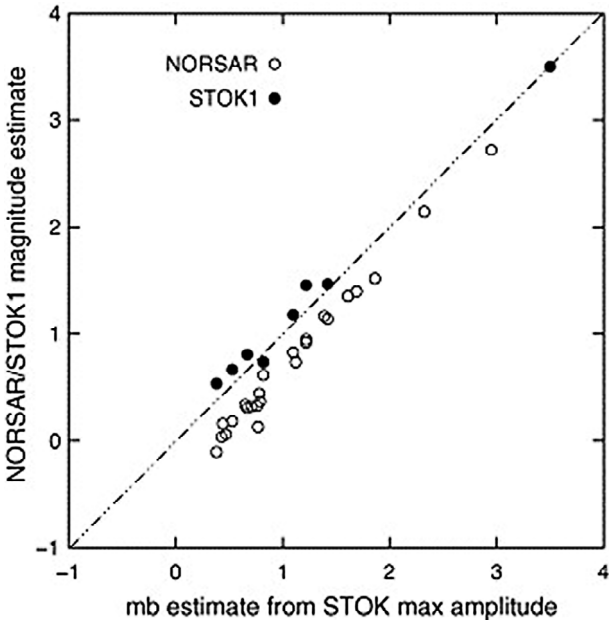

Fig. 9. Comparison of magnitudes estimated using maximum amplitudes at the STOK station (see Fig. 7) and those obtained using independent measurements on amplitudes at the temporary STOK1 station (see Fig. 8) and correlation and least squares inversion at the NORSAR array (described by *Gibbons and Ringdal*, 2006 and listed in Table 3). The magnitude of the main 24 June event is fixed to 3.50.

2000; *Waldhauser*, 2001). As we can see from Figs. 7, 8 and 10, the set of recordings at nearby stations is far from complete, the shortfall of data being compounded by a timing error for the STOK station prior to 10 June 2005. Only a single event in this sequence is in fact recorded by all three stations STOK, STOK1, and STOK2; this is the magnitude 0.8 event on 19 October 2005. The use of body waves for double-difference locations using the array recordings is precluded by the low SNR (cf. Fig. 5).

Schaff and Richards (2004a) point out that using the double-difference algorithm using differential travel-times for the high-amplitude *Lg* phase at a handful of regional stations can lead to relative epicenter estimates with a location precision on the order of 150 m. For each of the events listed in Table 3, a 30 s time-window of data for the *Lg* phase was extracted for all channels of each of the arrays displayed in Fig. 1. As *Schaff and Richards* (2004a) remark, since only relative time measurements are used, the precise start of the relatively long time-window is of secondary importance. These data segments were cross-correlated with waveform data for the intervals where the corresponding phase would be anticipated for all the other events, and relative delay times were estimated from the cross-correlation peaks. A low SNR at the array stations means that no meaningful time-delay measurement can be obtained for many event pairs at one or more of the stations.

Event pairs from the three largest events each record very clear correlation maxima for the *Lg* phase at the NOA, HFS, FIN and ARC arrays. The time-differences at the four stations lead to a system of equations which can be solved iteratively after the prescription of *Schaff and Richards* (2004a). With a phase velocity of 3.5 km/s^{-1}, a solution whereby events 7, 23 and 30 in Table 3 have relative locations of approximately (-20 m, -60 m), (0 m, 0 m) and (80 m, 100 m) appeared to be quite stable to small perturbations in the initial origin time and location estimates. Five other events also recorded acceptable correlation maxima at all four array stations; these time delays were added to the system of double-difference equations resulting in the relative location displayed in Fig. 11. To ensure the stability of this solution, relative locations were recalculated with events removed and initial epicenters and origin times perturbed in many different combinations.

Only the eight events whose relative locations are displayed in Fig. 11 could be located confidently using the differential travel times obtained from the *Lg*-phase correlations at the regional arrays. On each occasion whereby a new event was added, the system could be shown to result in a set of relative locations which were unstable to subsequent perturbations. The most likely reason for this is inaccuracy in the time-delay measurements for the low-SNR *Lg*-phases for these events. Care must always be taken in determining which cross-correlation time-delays are reliable and this usually requires conditions upon the correlation coefficient obtained. Fig. 3 of *Astiz et al.* (2000) illustrates analogous examples of cross-correlation traces where no well-defined maxima are determined. The stacking of correlation traces over the arrays performed in this study allows for far lower values of the correlation coefficient to be used than when only single stations are available. For example, *Astiz and Shearer* (2000) require a minimum correlation coefficient of at least 0.7 for a time differential from a given waveform pair to be included in the location inversion.

Whilst the solution displayed in Fig. 11 is limited to a small number of events, the pattern obtained is essentially consistent with the waveforms recorded at the STOK station (which was not used

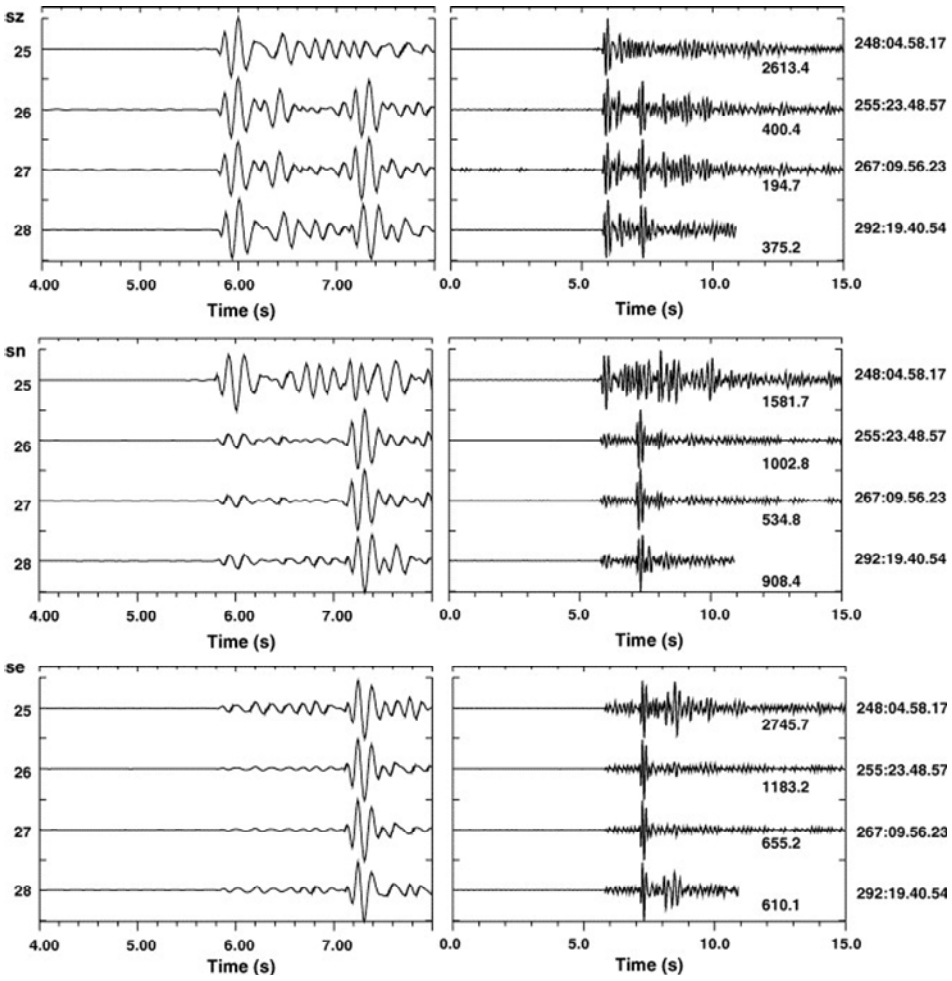

Fig. 10. Waveforms recorded at the STOK2 station for the times corresponding to the NORSAR correlation detections as listed in Table 3. sz, sn and se denote the short period vertical, north-south and east-west components respectively. Alignment in both left and right panels is based upon a maximum correlation with a 1.4 s time-window of the 24 September event starting at the P-arrival.

in this location calculation). The earliest events appear to have the smallest S-P differential travel times at STOK (see Fig. 7) which is consistent with marginally shorter distances to this station. The three largest events are approximately linearly aligned with the 24 June event most central and closer to the 28 April event than the 15 December event. This is consistent with the correlation coefficients given for the three event-pairs in Table 2.

5. The use of closely located seismic events for the rapid identification and correction of systematic timing errors

Rubin (2002) demonstrated how repeating seismic events could be exploited to correct high-precision earthquake catalogues for erroneous instrumental timing. *Gibbons* (2006) demonstrated how repeating events at a single site could be used to calculate a time-correction for a three-component seismic station using a second independent station as a control. *Gibbons and Ringdal* (2006) point out that timing anomalies on single instruments within a network or array are instantly revealed by a misalignment of the correlation maxima when forming the array beam. Exactly such a situation arose during the current study whereby two channels of the NORSAR array developed a timing disparity in the summer of 2005 due to a defective GPS receiver. Panel (a) of Fig. 12 shows the correlation peaks on selected channels of the NORSAR array (together with the beam from all 42 sites) from the correlation of the main shocks on 24 June and 28 April 2005. The master waveform template included both primary and secondary phases and was band-pass filtered in a wide frequency band; any differences in the times of maximum correlation at the different array sites resulting from small changes in the source-to-receiver paths are too small to be meas-

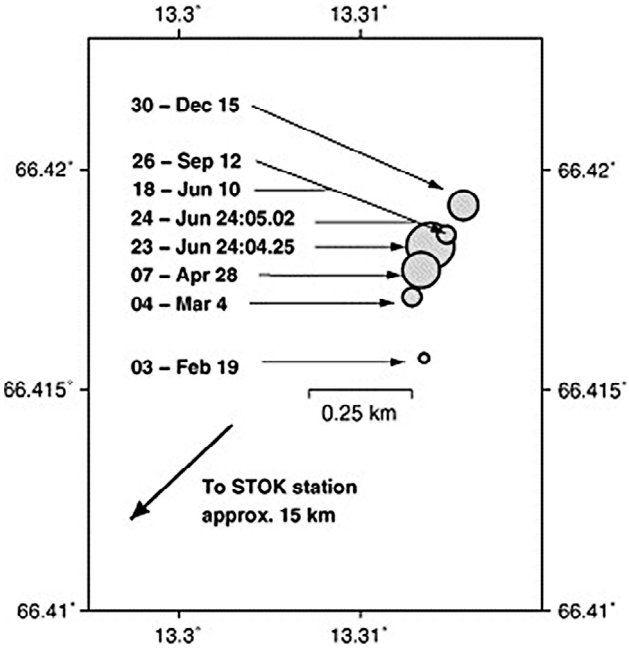

Fig. 11. Relative location estimates for eight of the events in Table 3 using only cross-correlation differential travel times for the Lg phases recorded at the NOA, HFS, FIN and ARC arrays. The solutions were obtained by iterating the double-difference equations as given in *Schaff and Richards* (2004a) using an Lg wave velocity of 3.5 km s^{-1}.

urable from this calculation. The elements NAO05 and NC601 produce a maximum correlation coefficient at times which are not consistent with the remaining array elements. The multi-channel cross-correlation and least squares method of *VanDecar and Crosson* (1990) is ideal for making accurate measurements of the time-delays involved. To the nearest 0.001 s, NC601 and NAO05 attain respectively a correlation maximum 0.538 s after and 1.723 s before the common correlation time.

The limitations of this method of time synchronization verification are clear; we require two events that have produced high SNR signals to have occurred sufficiently close to each other that waveform comparison produces a single significant maximum correlation peak. For a given array or network, it may be many weeks, months or years between the occurrence (if ever) of such fortuitous seismic events. Most other methods exploit waveform similarity between sensors, either for strong phase arrivals or for microseismic noise (see *Koch and Stammler*, 2003 and references therein); the exploitation of background noise is particularly helpful since it is not dependent upon the occurrence of satisfactory seismic events. However, the quality control illustrated in Fig. 12 is valid for an arbitrary configuration of stations (provided that all stations record both events sufficiently well) and requires neither coherence of a wavefront over a network or knowledge of the wavefield from a given source. Panel (b) of Fig. 12 illustrates the difficulty of measuring time discrepancies based upon even a strong teleseismic arrival. Whilst the elements NC601 and NAO05 are clearly anomalous, we can only deduce the timing discrepancy indirectly by measuring the relative delay times for each pair of channels and then judging which delays ought to be observed for the given incoming wavefront. The measurement of the relative delay times (cf. *VanDecar and Crosson*, 1990) is far more problematic with real seismic signals than with the symmetric correlation coefficient traces. Whereas the time of the peak of the correlation traces is largely independent of the frequency band applied, the signal coherency decreases dramatically with increasing frequency and relative time-delay measurements can vary greatly depending upon the choice of time-window. The plane wavefront models fail notoriously for the NORSAR array (see, for example, *Berteussen*, 1976) with little consensus as to what degree the observed anomalies are the result of local effects or distant heterogeneities (e.g. *Pritchard et al.*, 2000). The locations of the markers relative to the features on the waveforms in panel (b) of Fig. 12 illustrate the shortcomings of the best-fit plane-wave model.

An additional problem can be observed for the SPB3 instrument of the Spitsbergen array in Fig. 12(c), which is also the result of a defective GPS receiver. The correlation between these two very low SNR signals is more than sufficient to identify the problem but too poor to be able to calculate a high-precision estimate for the timing anomaly. A similar phenomenon was observed on one channel of the FINES array.

A comparison between the differential reference times obtained by correlation at the array stations (Table 4) and the differential times obtained at the STOK station confirm the known drift (to within approximately 0.3 s) which occurred at this station as the result of a GPS receiver problem prior to June 2005. Unfortunately, without additional instruments closeby, we are not able to measure directly this drift using these reference events. The calculation of the timing discrepancy on the NORSAR array was possible since the delays on all but 2 of the 42 sites were

measured to zero to the limit of the accuracy permitted by the available waveforms. Since the separation between sites in the array is small compared with the distance between source and receiver, the change in S-P time-differentials is similar over the array. We would only be able to measure the drift at the STOK Station directly if another station were present sufficiently close to STOK that the differences in S-P time-differentials between the two stations were negligible. However, in a multi-event hypocenter location solution, where the S-P times from the STOK station are given high weights and the absolute time picks are given a high uncertainty value, a reasonable estimate of the drift at the time of each of the events located should be possible.

6. Conclusions

We have identified five seismic events exceeding magnitude 2.0 which occurred in the Rana region of northern Norway during the calendar year 2005; these were the only such events from this region during this period to be detected by more than one IMS seismic station, all of which are at distances in excess of 600 km. Three of the events, including the largest (magnitude 3.5 on 24 June 2005), generated very similar signals at the IMS array stations; 3 min long waveform segments at the large aperture NORSAR array resulted in very high correlation coefficients even when bandpass filtered between 3 and 8 Hz. In an attempt to find further seismic events of lower magnitude from the vicinity of the source of the largest event, an on-line correlation detector was initiated using the waveforms generated by this event, recorded at the NORSAR array, as a signal template. When run on continuous NORSAR data for the whole of 2005, a total of 32 clear detections were made. Only three of these detections occurred at times when a signal detectable by traditional energy detectors was observed at the NORSAR array.

The validity of 30 of these correlation detections was confirmed beyond reasonable doubt by applying similar correlation detectors to the other Nordic IMS array stations; all but two of the matched filter detections at NORSAR occurred within a small fraction of a second of an independent, corresponding detection at least one of the other arrays. Thirty-one out of the 32 detections are confirmed to correspond to low magnitude events in the Rana region by closer stations of the Norwegian National Seismic Network (NNSN); the remaining detection at NORSAR is presumed to be a false alarm. Many of the correlation detections occurred during the coda of the largest events. The synchronicity of these subsequent detections at each of the different arrays indicated that these probably corresponded to distinct small aftershocks and this was duly confirmed by examining the data from the local stations.

Many of these coda events were missed if too short a waveform template was used; the signal template should include the part of the wavetrain containing the greatest amplitudes. When using conventional energy detectors, the start of the signal is the most important since this is where the highest SNR is observed (STA/LTA detectors are optimal for impulsive signals). Correlation detectors work by the recognition of waveforms and are unaffected by the SNR in the STA/LTA sense; only the ratio of the signal amplitude to the background noise is important. They are consequently as effective with emergent signals as with impulsive signals and there may be many cases whereby the optimal template for detecting an event at a given station does not include the initial arrivals. The template used for the initial study consisted of 120 s of data for each channel, a somewhat arbitrarily chosen length. Subsequent runs have been performed with longer templates (e.g. 180 s) which include the full *Lg* coda although, for this case, no additional events were detected.

Although the recordings of the sequence by the local network are very incomplete, the signals that exist are of a very high quality and indicate that events detected clearly by the distant NORSAR array are of magnitudes as low as 0.5. This is significant for two reasons. Firstly, this represents at least an order of magnitude improvement in the detection capability for the network of arrays. (In practice, the effective improvement in detection capability is even greater since even events of magnitudes 2.0 at this distance are only detected with confidence by the ARCES array and may thus be associated with a large location error.) Secondly, the events were detected using a signal template from an event three orders of magnitude larger.

The incompleteness of the local network re-

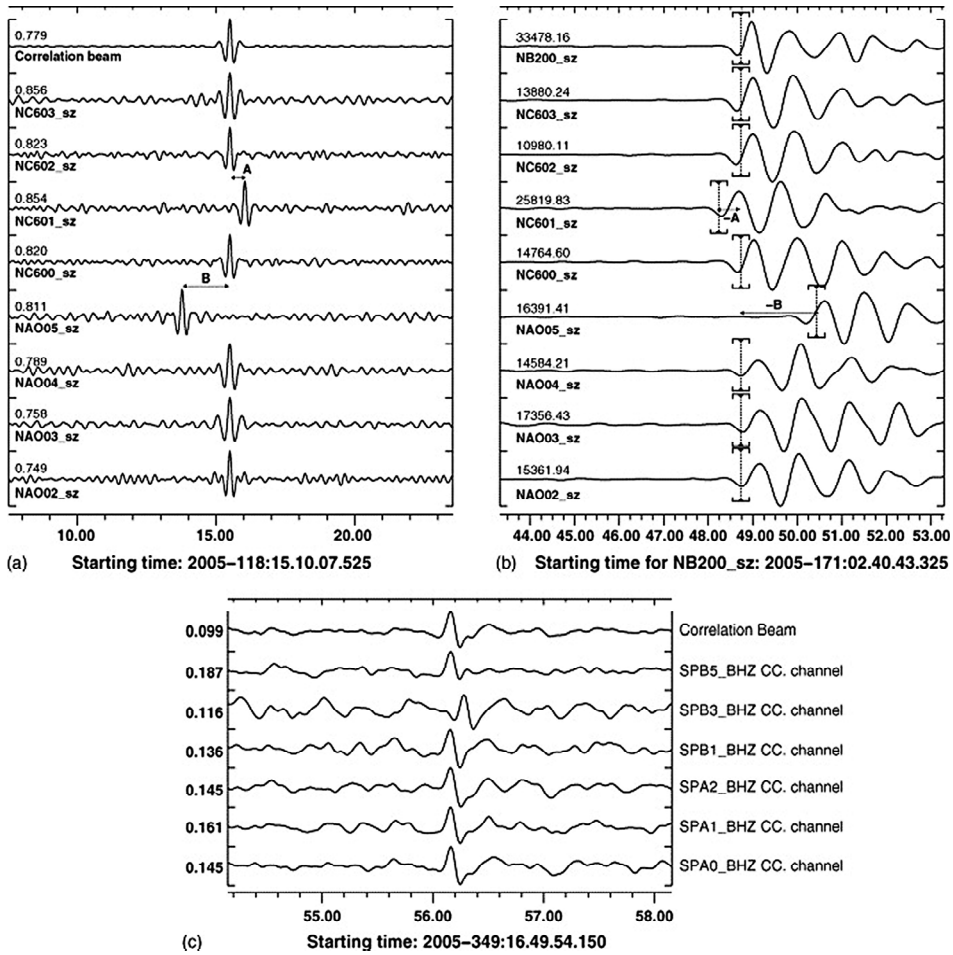

Fig. 12. Exploitation of repeating seismic events for the identification and measurement of timing discrepancies between sites of an array or network. (a) Displays correlation coefficient traces for 8 of the 42 short period vertical channels of the NORSAR array (together with the correlation beam) for a 15 s long time-segment on 28 April 2005, where the master signal template consists of 120.0 s long data segments extracted from the main 24 June 2005 event, filtered between 2.0 and 12.0 Hz. To within the time resolution available, all channels achieve a maximum correlation coefficient simultaneously except for sites NC601 and NA005; these differ from the common correlation time by delays labelled A and B, respectively. (b) Shows a P-arrival from a large teleseismic event on 21 June 2005 (origin time according to United States Geological Survey 02.32.59.97: latitude 36.35°, longitude 71.08°, depth 235 km, m_b = 5.2; see http://www.neic.usgs.gov/neis/epic/epic-mct.html) which reaches the NB200 central element at a time 2005-171:02.40.47.875. The remaining channels are delayed according to the best-fit, uncorrected, plane wavefront and the markers indicate the relative times deduced from the maximum correlation times in (a). Waveforms are bandpass-filtered between 0.8 and 2.0 Hz. (c) Shows aligned correlation coefficient channels on the SPITS array using the 24 June Mo i Rana event as a master signal. SPB3 is clearly anomalous by a fraction of a second.

cordings precludes a comprehensive double-difference location of the full set of events. However, cross-correlation time-delay measurements using the *Lg* phase at the array stations, together with the double-difference iteration procedure of *Schaff and Richards* (2004a), allows for a stable relative location estimate involving eight of the events. Both the local network recordings and the delay-times obtained by *Lg* cross-correlation at the array stations indicate a maximum epicenter separation of below 0.5 km.

We have demonstrated additionally that events which are as closely located as those in this sequence can be exploited to expose systematic timing anomalies which effect one or more sites within an array or network. When such repeating seismic events occur, highly accurate measurements of the timing discrepancy can be made without the need to calibrate for the observed arrival pattern of the incoming wavefront.

7. Discussion and recommendations

We purposefully restricted the current study to seismicity in this very limited region occurring during the calendar year 2005. The whole region has demonstrated regular seismic activity for as long as it has been observed (see, for example, *Hicks et al.*, 2000 and references therein) and there is a high possibility that many more occurrences of similar events from this region would be identified by continuing the detection process both back-

wards and forwards in time. The waveform correlation detector described in this paper is now run continuously on all incoming NORSAR data and, already within the first 3 months of 2006, three almost co-located events were detected and confirmed by stations of the NNSN (origin times of 2006-056:23.14.49.050, 2006-068:20.52.58.800 and 2006-085:08.03.53.425). Of the five events in this region during 2005 which were clearly detected by the IMS arrays (see Table 1), two events, numbers 7872 and 8368, were found to be unrelated to the remaining three and were not detected using the waveform template for event 8033. Waveform templates were also extracted for these events and produced a number of correlation detections. Event 7872 corresponded to a number of events in the earthquake catalogue for the University of Bergen (for example, 2005-097:16.19.50 and 2005-104:06.54.24). Event 8368 corresponded to confirmed earthquakes with origin times 2005-081:20.40.27 and 2005-322:11.07.18, in addition to an aftershock 4 h after the master event and numerous events in May 2006.

The seismicity in the greater Rana region has been demonstrated by *Hicks et al.* (2000) to occur in many different geographical clusters and, based on the current work alone, it is impossible to tell whether the waveform similarity (and hence event detectability) observed here will be equally applicable to other regions of Nordland, let alone in the even wider global context. In addition to the problem of geographical portability, there is the question of how the performance of such detectors would vary with the recording network available. The situation in the current paper is as close to ideal for this task as is possible; there is no region on earth with a greater density of IMS array stations, backed up by a national network of seismometers to confirm the findings. The hypothesis of *Gibbons and Ringdal* (2006) that such methods, when applicable, ought to reduce the detection threshold by approximately an order of magnitude appears to hold still; the detection of the 28 April and 15 December events on the Spitsbergen array at over 1300 km is as important in the context of explosion monitoring as the detection of the numerous small tremors and aftershocks by the array stations at half that distance.

Also of great interest to the field of seismic monitoring is the ability to detect earthquake aftershocks even within the coda of events well in excess of an order of magnitude larger using only a single array station. *Richards and Kim* (1997) pointed out that a clear aftershock following the 16 August 1997, magnitude 3.5, Kara Sea event made it highly unlikely that the event had been a clandestine explosion as was originally hypothesized. If a correlation detector can resolve one or more clear aftershocks from the incoherent coda as was demonstrated in Fig. 5, this could constitute a rapid and significant step in the source discrimination process.

Correlation detectors were employed at the regional Fennoscandian array stations over short time segments to verify the validity of detections made at the NORSAR array. However, a single preliminary attempt to perform the full continuous process at ARCES resulted in a huge number of detections, the majority of which clearly did not correspond to events in the Rana region.

This phenomenon is characteristic of the regional seismic arrays (see *Gibbons and Ringdal*, 2006) and occurs simply because of the high coherence of the actual waveforms between sensors. (This problem is largely avoided on large arrays and networks.) In the case study examined by *Gibbons and Ringdal* (2006), almost all of these false alarms were eliminated by detecting a "non-zero apparent velocity" in the actual correlation coefficient traces. That elementary test is more difficult to apply when using long time windows as in the example here simply because the correlation maxima are unlikely to be dominated by the contribution from one single short time-window, and so degrading the validity of the plane-wave assumption which made the technique so successful in *Gibbons and Ringdal* (2006). The same principles will still be able to be applied but more care must be taken to identify exactly which parts of the time-series dominate the correlation coefficient, and use these shorter time windows for estimating the apparent velocity.

The accurate relocation of a small number of events using temporary stations at local distances and cross-correlation differential travel time measurements can facilitate a calibration for more distant stations which can lead to a dramatic improvement in the accuracy of subsequent location estimates by conventional means. Fig. 6 shows the original location estimate for the 24 June 2005, event from Table 1 together with the relocation performed using the local network. The error ellip-

ses associated with the locations of seismic events are likely to increase with decreasing event magnitude because the decreasing SNR of the signals will lead to greater errors in arrival time picks and slowness and azimuth measurements. However, the improved event locations for certain regions may allow correction for some of the systematic bias in the array-only estimates. The event is mislocated by approximately 20 km to the East, which is not very surprising given the azimuth coverage of the Fennoscandian array stations. The mislocation is consistent with the slowness estimate biases observed by *Schweitzer* (2001b); see also *Kværna et al.* (2005). In situations where events are only well observed by a single array station, the application of carefully calibrated travel time and azimuth corrections may lead to a dramatic improvement in location estimates (*Gibbons et al.*, 2005).

It is unclear as to how long the STOK1 and STOK2 stations will remain in the field. It was originally intended that they be removed during the summer of 2006, but this decision may be overturned in the light of the excellent recordings which have been produced of small seismic events in various clusters in the Rana region.

These stations, together with the permanent Stokkvågen station, STOK, have permitted a far greater event location accuracy than has been available previously. Many events both prior to and following the placement of the temporary network may now be better constrained by considering waveform similarity at regional distances with the accurately located events from this period. Financial limitations prevent the installation of stations close to every site with seismicity of interest. This work may be of interest to the monitoring of small earthquakes in remote regions where it is logistically difficult or prohibitively expensive to maintain a permanent local network.

We recommend that a large-scale effort be made to continue the identification of repeating seismic sources in line with the work of *Schaff and Waldhauser* (2005). This will serve the manifold purposes of increasing our knowledge of the distribution of seismicity, reducing the detection threshold for low-magnitude seismic events, obtaining more accurate location estimates, and providing large banks of test events with which continual quality control of instrumental timing can be carried out.

The availability of historical recordings from seismic stations is essential if the accumulating database of seismic recordings is to be best utilized for the detection and interpretation of subsequent seismic events. The large-aperture NORSAR array is demonstrably not well-suited to the detection and identification of weak regional seismic phases using conventional energy detectors, which is the current emphasis in the field of nuclear explosion monitoring. It has been argued, therefore, that a spatial redesign of the array would make it a more useful IMS station. Given the now 35 year history of high-quality digital seismic data from NORSAR, containing one of the most comprehensive archives of nuclear explosion recordings in existence, the increasing importance of waveform correlation detectors offers the strongest possible argument against a relocation of sites within the array.

The improvement in event detectability with an increasing number of sensors in an array (irrespective of array geometry) is usually greater for correlation detectors than the corresponding improvement for energy detectors. This is because, for traditional array processing, additional sensors only improve the SNR significantly if the new channel reinforces the observed signal and simultaneously suppresses noise (see, for example, *Kværna*, 1989). For the correlation detectors, the condition of waveform coherence over the array is replaced with the condition of waveform similarity between the signal template and the incoming data stream (*Gibbons and Ringdal*, 2006) and this means that additional sensors at essentially arbitrary positions can (provided that the single-channel SNR is not significantly worse) only improve the array correlation beam. We have observed in this paper that a reduction in the number of array elements at a given distance does reduce the detectability using waveform correlation and we conclude that the newer nine-site regional arrays in the IMS will provide less effective correlation detectors than the older arrays with a greater number of sites and a larger aperture.

Acknowledgements

This material is based upon work supported by the Department of Energy (National Nuclear Security Administration) under Award Number DE-FC52-05NA26604. The Norwegian National

Seismic Network is operated by the Department of Earth Science, University of Bergen, Norway and supported by Oljeindustriens Lands Forening (OLF) and the Faculty of Mathematics and Natural Sciences, University of Bergen. We are grateful to Jens Havskov and Kuvvet Atakan for valuable discussions regarding seismicity in the Rana region. We are also grateful to two referees for very thoughtful and thorough reviews of this paper. We are especially grateful for the suggestion of applying the *Lg* double-difference algorithm of *Schaff and Richards* (2004a). Maps were created using GMT Software (*Wessel and Smith*, 1995).

References

Astiz, L., Shearer, P.M., 2000. Earthquake locations in the inner continental borderland, offshore southern California. Bull. Seism. Soc. Am. 90,425-449.

Astiz, L., Shearer, P.M., Agnew, D.C., 2000. Precise relations and stress change calculations for the Upland earthquake sequence in southern California. J. Geophys. Res. 105, 2937-2953.

Atakan, K., Lindholm, C.D., Havskov, J., 1994. Earthquake swarm in steigen, northern norway: an unusual example of intraplate seismicity. Terra Nova 6, 180-194.

Berteussen, K.A., 1976. The origin of slowness and azimuth anomalies at large arrays. Bull. Seism. Soc. Am. 66, 719-741.

Bungum, H., Hokland, B.K., Husebye, E.S., Ringdal, F., 1979. An exceptional intraplate earthquake sequence in meløy, northern norway. Nature 280, 32-35.

Bungum, H., Husebye, E.S., Ringdal, F., 1971. The NORSAR array and preliminary results of data analysis. Geophys. J. R. astr. Soc. 25, 115-126.

Geller, R.J., Mueller, C.S., 1980. Four similar earthquakes in central California. Geophys. Res. Lett. 7 (10), 821-824.

Gibbons, S.J., 2006. On the identification and documentation of timing errors: an example at the KBS Station. Spitsbergen. Seism. Res. Lett. 77, 559-571.

Gibbons, S.J., Kværna, T., Ringdal, F., 2005. Monitoring of seismic events from a specific source region using a single regional array: a case study. J. Seismol. 9, 277-294.

Gibbons, S.J., Ringdal, F., 2006. The detection of low magnitude seismic events using array-based waveform correlation. Geophys. J. Int. 165, 149-166 doi: 10.1111/j.1365-246X.2006.02865.x.

Harris. D.B., 1991. A waveform correlation method for identifying quarry explosions. Bull. Seism. Soc. Am. 81, 2395-2418.

Hicks, E.C., Bungum, H., Lindholm, C.D., 2000. Seismic activity, inferred crustal stresses and seismotectonics in the Rana region, northern Norway. Quater. Sci. Rev. 19, 1423-1436.

Kennett, B.L.N., 2002. The Seismic Wavefield. Vol. II. Interpretation of Seismograms an Regional and Global Scales. Cambridge University Press.

Koch, K., Stammler, K., 2003. Detection and elimination of time synchronization problems for the GERESS array by correlating microseismic noise. Seism. Res. Lett. 74 (6), 803-816.

Kværna, T., 1989. On exploitation of small-aperture NORESS type arrays for enhanced P-wave detectability. Bull. Seism. Soc. Am. 79, 888-900.

Kværna, T., Gibbons, S.J., Ringdal, F., Harris, D.B., 2005. Integrated seismic event detection and location by advanced array processing. In: Proceedings of the 27th Seismic Research Review, Rancho Mirage on Groundbased Nuclear Explosion Monitoring Technologies California, September, 2005, pp. 927-936.

Massa, M., Ferretti, G., Spallarossa, D., Eva, C., 2006. Improving automatic location procedure by waveform similarity analysis: an application in the South Western Alps (Italy). Phys. Earth Planet. Inter. 154, 18-29.

Menke, W., 2001. Using waveform similarity to constrain earthquake locations. Bull. Seism. Soc. Am. 89 (4), 1143-1146.

Mykkeltveit, S., Ringdal, F., 1981. Phase identification and event location at regional distances using small-aperture array data. In: Husebye, E.S., Mykkeltveit, S. (Eds.), Identification of Seismic Sources-Earthquake or underground explosions. Reidel Publishing Company, pp. 467-481.

Nakahara, H., 2004. Correlation distance of waveforms for closely located events. I. Implications of the heterogeneous structure around the source region of the 1995 Hyogo-Ken Nanbu, Japan, earthquake ($M_w = 6.9$). Geophys. J. Int. 157, 12551268.

Poupinet, G., Ellsworth, W.L., Frechet. J., 1984. Monitoring velocity variations in the crust using earthquake doublets: an application to the Calaveras Fault. Calif. J. Geophys. Res. 89, 5719-5731.

Pritchard, M.J., Foulger, G.R., Julian, B.R., Fyen, J., 2000. Constraints on a plume in the mid-mantle beneath the Iceland region from seismic array data. Geophys. J. Int. 143, 119-128.

Richards, PG., Kim, W.-Y., 1997. Testing the nuclear testban treaty. Nature 389, 781-782.

Richards, P.G., Waldhauser, F., Schaff, D., Kim, W.-Y., 2006. The applicability of modern methods of earthquake location. Pure Appl. Geophys. 163, 351-372.

Ringdal, F., Kværna, T., 1989. A multi-channel processing approach to real time network detection, phase association, and threshold monitoring. Bull. Seism. Soc. Am. 79, 1927-1940.

Riviere-Barbier, F., Grant, L.T., 1993. Identification and location of closely spaced mining events. Bull. Seism. Soc. Am. 83, 15271546.

Rubin, A.M., 2002. Using repeating earthquakes to correct high-precision earthquake catalogs for time-dependent station delays. Bull. Seism. Soc. Am. 92, 1647-1659.

Schaff, D.P., Richards, PG., 2004. Lg-wave cross correla-

tion and double-difference location: application to the 1999 Xiuyan, China. Seq. Bull. Seism. Soc. Am. 94, 867-879.

Schaff, D.P., Richards, P.G., 2004. Repeating seismic events in China. Science 303, 1176-1178.

Schaff, D.P., Waldhauser, F., 2005. Waveform cross-correlation-based differential travel-time measurements at the northern California Seismic Network. Bull. Seism. Soc. Am. 95, 2446-2461.

Schaff, D.P., Waldhauser, F., 2006. Improving magnitude detection thresholds using multistation, multievent, and multiphase methods. In: Proceedings of the 28th Seismic Research Review on Ground-based Nuclear Explosion Monitoring Technologies. Orlando, Florida, September 2006, pp. 493-502.

Schweitzer, J., 2001. HYPOSAT - an enhanced routine to locate seismic events. Pure Appl. Geophys. 158, 277-289.

Schweitzer, J., 2001b. Slowness corrections - one way to improve idc products. Pure Appl. Geophys. 158, 375-396.

Shearer, P.M., 1997. Improving local earthquake locations using the L 1 norm and waveform cross correlation: application to the Whittier Narrows, California, aftershock sequence. J. Geophys. Res. 102, 8269-8283.

VanDecar, J.C., Crosson, R.S., 1990. Determination of teleseismic relative phase arrival times using multi-channel cross-correlation and least squares. Bull. Seism. Soc. Am. 80, 150-169.

Waldhauser, F., 2001. HypoDD - a program to compute double-difference hypocenter locations. Tech. Rep. Open-File Report 01-113, U.S. Geological Survey.

Waldhauser, F., Ellsworth, W.L., 2000. A double-difference earthquake location algorithm: method and application to the Northern Hayward Fault, California. Bull. Seism. Soc. Am. 90 (6), 1353-1368.

Wessel, P., Smith, W.H.F., 1995. New version of the generic mapping tools. EOS Trans. Am. Geophys. Union 76, 329.